Geometry-induced protein pattern formation

Dominik Thalmeier[a,b,c,d], Jacob Halatek[a,b], and Erwin Frey[a,b,1]

[a]Arnold Sommerfeld Center for Theoretical Physics, Ludwig-Maximilians-Universität München, D-80333 Munich, Germany; [b]Center for NanoScience, Ludwig-Maximilians-Universität München, D-80333 Munich, Germany; [c]Donders Institute, Radboud University, 6525 EZ Nijmegen, The Netherlands; and [d]Department of Biophysics, Radboud University, 6525 AJ Nijmegen, The Netherlands

Edited by Herbert Levine, Rice University, Houston, TX, and approved December 9, 2015 (received for review August 4, 2015)

Protein patterns are known to adapt to cell shape and serve as spatial templates that choreograph downstream processes like cell polarity or cell division. However, how can pattern-forming proteins sense and respond to the geometry of a cell, and what mechanistic principles underlie pattern formation? Current models invoke mechanisms based on dynamic instabilities arising from nonlinear interactions between proteins but neglect the influence of the spatial geometry itself. Here, we show that patterns can emerge as a direct result of adaptation to cell geometry, in the absence of dynamical instability. We present a generic reaction module that allows protein densities robustly to adapt to the symmetry of the spatial geometry. The key component is an NTPase protein that cycles between nucleotide-dependent membrane-bound and cytosolic states. For elongated cells, we find that the protein dynamics generically leads to a bipolar pattern, which vanishes as the geometry becomes spherically symmetrical. We show that such a reaction module facilitates universal adaptation to cell geometry by sensing the local ratio of membrane area to cytosolic volume. This sensing mechanism is controlled by the membrane affinities of the different states. We apply the theory to explain AtMinD bipolar patterns in Δ EcMinDE *Escherichia coli*. Due to its generic nature, the mechanism could also serve as a hitherto-unrecognized spatial template in many other bacterial systems. Moreover, the robustness of the mechanism enables self-organized optimization of protein patterns by evolutionary processes. Finally, the proposed module can be used to establish geometry-sensitive protein gradients in synthetic biological systems.

cell polarity | Min system | geometry sensing | pattern formation | nonlinear dynamics

Protein patterns serve to initiate and guide important cellular processes. A classic example is the early patterning of the *Drosophila* embryo along its anterior–posterior axis (1). Here, maternal morphogen gradients initiate a complex patterning process that subsequently directs cell differentiation. However, protein patterns play a regulatory role even at the single-cell level. For example, they determine cell polarity and the position of the division plane. In the yeast *Saccharomyces cerevisiae*, the GTPase Cdc42 regulates cell polarization, which in turn determines the position of a new growth zone or bud site. This pattern-forming process is driven by the interaction between a set of different proteins that cycle between the plasma membrane and the cytoplasm (2, 3). In the rod-shaped bacterium *Escherichia coli*, Min proteins accumulate at the ends of the cell to inhibit the binding of the division proteins (4, 5). Here, the main player in the pattern-forming process is the ATPase MinD. It attaches to the membrane in its ATP-bound state and recruits MinE and further MinD-ATP from the cytosol (6). Cycling of proteins between membrane and cytosol is mediated by the action of MinE, which stimulates the intrinsic ATPase activity of MinD and thereby initiates its detachment. The ensuing oscillatory pattern directs the division machinery to midcell, enabling proper cell division in two viable daughter cells.

In all of these processes, regulatory proteins establish chemical gradients or patterns that reflect aspects of cell shape. However, how is gradient or pattern formation achieved in the absence of an external template? Many possible mechanisms have been proposed and they are by no means fully classified yet (7, 8). Establishing a pattern involves definition of preferred accumulation points and requires that the symmetry of the homogeneous state is broken. In *Bacillus subtilis*, there is good evidence suggesting that DivIVA recognizes negative membrane curvature directly by a mechanism that is intrinsic to this cell division protein (7, 9). In contrast, enrichment of MinD at the cell poles in *E. coli* is an emergent property of the collective dynamics of several proteins. As shown in refs. 10–16, the nonlinear dynamics of the Min system leads to a polar pattern, which oscillates along the long axis and is clearly constrained by cell geometry. A clear disadvantage of such self-organized symmetry breaking through a dynamical instability is that the kinetic parameters must be fine-tuned to allow the establishment of a stable polar pattern.

Here, we show that cell geometry itself can enforce a broken symmetry under generic conditions without any need for fine-tuning. We introduce a class of geometry-sensing protein systems whose only stable state is a spatial pattern that is maintained by energy consumption through an ATPase or GTPase (NTPase). The proposed mechanism is based on a generic property of diffusion: The probability that a protein diffusing through the cytosol will strike (and attach) to the membrane scales with the area of membrane accessible to it. Thus, close to the poles of a rod-shaped cell, most of the trajectories available lead to the membrane. Close to midcell, where the membrane is almost flat, about one-half of the possible paths lead away from the membrane. However, on its own, this mechanism only produces transient patterns on the membrane, as the system approaches a stable, uniform equilibrium in finite time (17). Moreover, patterns only emerge from specific initial conditions. In this paper, we ask, how can this generic property of diffusion be complemented by a minimal set of biomolecular processes to robustly maintain patterns? We show that the NTPase activity of a single protein that cycles between membrane and cytosol is sufficient to achieve this goal. Our analysis

Significance

Biological cells need the ability to guide intracellular processes to specific spatial locations. This requires biochemical processes to sense and adapt to the geometry of the organism. Previously suggested mechanisms either assume proteins that are able to directly sense membrane curvature or are based on nonlinear diffusion–reaction systems that can generate geometry-adapted patterns. The latter, however, requires fine-tuning of the reaction rates. Here, we show that geometry adaption already follows from generic chemical dynamics. We present a simple reaction module based on generic reactions that establishes geometry-dependent patterns robustly without the need to tune kinetic rates nor any explicit curvature-sensing mechanism.

Author contributions: D.T., J.H., and E.F. designed research, performed research, and wrote the paper.

The authors declare no conflict of interest.

This article is a PNAS Direct Submission.

Freely available online through the PNAS open access option.

[1]To whom correspondence should be addressed. Email: frey@lmu.de.

This article contains supporting information online at www.pnas.org/lookup/suppl/doi:10.1073/pnas.1515191113/-/DCSupplemental.

shows that an inhomogeneous density profile is established on the membrane in the generic case where the affinities of NTP- and NDP-bound forms differ. Moreover, these membrane-bound patterns are amplified if the proteins are able to bind cooperatively to the membrane (e.g., due to dimerization). This mechanism is highly robust because the stable, uniform equilibrium is simply replaced by a unique, stable patterned state. In particular, the mechanism involves no dynamical instability and requires no fine-tuning of parameters.

Experimental support for the proposed mechanism comes from *E. coli* mutants in which both EcMinD and EcMinE were replaced by chloroplastic AtMinD (MinD homolog from *Arabidopsis thaliana*) (18). With this single ATPase (19) the system establishes a bipolar pattern along the long axis, rescuing the ΔMinDE mutant from cell division pathologies. Mutation studies of the Walker-A binding module show that AtMinD (unlike EcMinD) can form dimers on the membrane even in its ADP-bound form (19–21), suggesting that both forms can cooperatively bind to the membrane. Our study shows that such cooperativity leads to a bipolar pattern along the long axis of the cell, as observed. Furthermore, we suggest that, due to its generic nature, the binding module might also play an essential role in other bacterial pattern-forming systems.

A Generic Reaction Module for Sensing of Cell Geometry

We consider a reaction module comprised of a single type of NTPase that cycles between an NDP-bound (P_{NDP}) and a NTP-bound (P_{NTP}) state (Fig. 1*A*). Both forms are allowed to freely diffuse in the cytosol and the membrane with diffusion constants D_c and D_m, respectively. For the biochemical reaction kinetics, we assume that (*i*) cytosolic P_{NDP} undergoes nucleotide exchange with a rate λ; (*ii*) both protein species can bind to the membrane with respective attachment rates ω_D^+ and ω_T^+; (*iii*) in addition to direct membrane attachment, each protein species can also bind cooperatively to the membrane, forming homodimers, with corresponding recruitment rates k_{dD} for P_{NDP} and k_{tT} for P_{NTP}; (*iv*) hydrolysis of P_{NTP} triggers detachment with rate ω_t^-, which is thus converted into cytosolic P_{NDP}; (*v*) membrane-bound P_{NDP} is released to the cytosol with detachment rate ω_d^-. For a mathematical formulation in terms of reaction–diffusion equations, please refer to *SI Appendix*, Eqs. **1–6**.

This reaction module serves as a model for the bipolar pattern of AtMinD in *E. coli* cells (18): AtMinD is an ATPase (19) that has been reported to dimerize (19, 21). This process thus provides evidence for cooperative membrane binding. Unlike EcMinD (20), AtMinD dimerizes even when its Walker-A binding module is inactivated (19), locking the protein in its ADP-bound state. This strongly suggests that also the ADP-bound form of AtMinD exhibits cooperative membrane binding, as we have assumed in the above reaction scheme by introducing a recruitment rate k_{dD} for P_{NDP}. Overall, there is strong evidence that AtMinD shows the same interactions with the membrane as EcMinD but with additional cooperative membrane binding in its ADP-bound state.

If not mentioned otherwise, we use the following model parameters, which are set to experimental values acquired for *E. coli*, if available. The diffusion constants in the cytosol and on the membrane are set to $D_c = 16\ \mu m^2/s$ and $D_m = 0.013\ \mu m^2/s$, respectively (22, 23). The nucleotide exchange rate is set to $\lambda = 6\ s^{-1}$ (15) to meet the lower bound of $3\ s^{-1}$ (22). The kinetic parameters are chosen to be of the order of 1 μm/s for attachment, $1\ s^{-1}$ for detachment, and $0.1\ \mu m^2/s$ for recruitment (15); for the specific values, see *SI Appendix*, Table 1. In the numerical studies, the cell shape is modeled as a 2D ellipse. (Remark: For the sake of clarity, we will still use the terms of cytosolic volume and membrane area instead of areas and lengths.) This reduced geometry has the same basic symmetries as the real geometry of an *E. coli* cell. Importantly, in contrast to a 1D model, it fully accounts for the different dimensionalities of cytosol and membrane. This will turn out to be essential for the ability of the system to generate protein patterns that reflect cell geometry. The overall protein density is set to a physiologically typical value of the order of 1 μM (24). For a cell which is 5 μm long and has a width of 1 μm, this gives a fixed protein number of about 2,000 MinD molecules. Specifically, in our numerical studies, we set the protein density in the bulk to be $\rho = 500\ \mu m^{-2}$ if all proteins are in the cytosol. To accommodate changes in cell size, we keep this mean density constant and change the number of proteins as appropriate.

Results

The Impact of Cell Geometry on Protein Gradients in Elongated Cells. We performed a numerical analysis of this reaction module, paying particular attention to the effect of varying the cell geometry and the degree of cooperativity in membrane binding (Fig. 1*B*). Our simulations show that, in elongated cells, the protein density on the membrane is always inhomogeneous and reflects the local cell geometry. Indeed, one can show analytically that the homogeneous steady state ceases to exist as one passes from circular to elliptical geometry (cf. *SI Appendix*). We observe

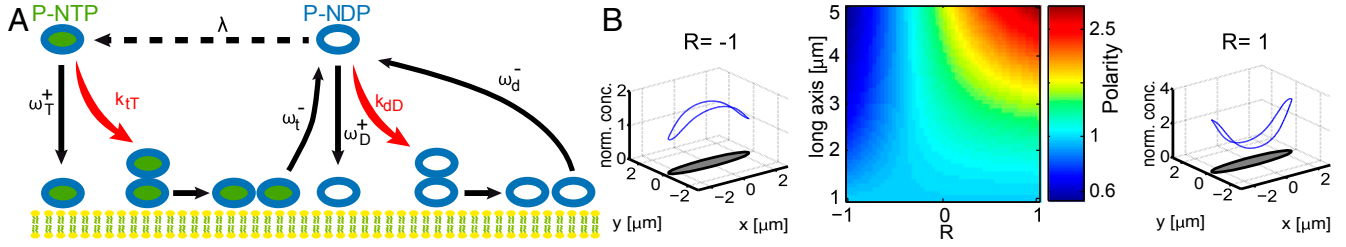

Fig. 1. Minimal reaction module for geometry-induced cell polarity. (*A*) Illustration of the reaction module: cytosolic P_{NDP} can exchange its nucleotide, $P_{NDP} \rightarrow P_{NTP}$, with rate λ. P_{NTP} attaches to the membrane with rate ω_T^+ where it recruits further P_{NTP} with rate k_{tT}. At the membrane, hydrolysis triggers detachment with rate ω_t^- such that membrane-bound P_{NTP} is converted to cytosolic P_{NDP}. Cytosolic P_{NDP} attaches to the membrane with rate ω_D^+ where it recruits further P_{NDP} with rate k_{dD} or detaches with rate ω_d^-. (*B*) Membrane-bound proteins accumulate either at midcell (*Left*) or form a bipolar pattern with high protein densities at the cell poles (*Right*). The *Left* and *Right* plots show the normalized concentration of the membrane density (blue curve) and the corresponding geometry of the cell (gray ellipse). The membrane density of the protein is divided by its minimum concentration (*Left*: $113\ \mu m^{-1}$; *Right*: $100\ \mu m^{-1}$) such that the minimum of the normalized density is 1. The polarity *P* (color bar in plot is logarithmically spaced) of the pattern strongly depends on cell geometry and preference *R* for the recruitment of a certain nucleotide state (*Middle*); the length of the short axis is fixed at $l = 1$ μm, and we have used $k_{dD} + k_{tT} = 0.1$ μm/s. While for large *R* (preferential recruitment of P_{NDP}) the proteins form a bipolar pattern on the membrane, the membrane-bound proteins accumulate at midcell for small *R* (preferential recruitment of P_{NTP}). If the recruitment processes are balanced ($R = 0$), the pattern is flat and polarity vanishes. The cell geometry determines how pronounced a pattern becomes: the more elongated the ellipse, the more sharply defined the pattern, whereas it vanishes completely when the ellipse becomes a circle.

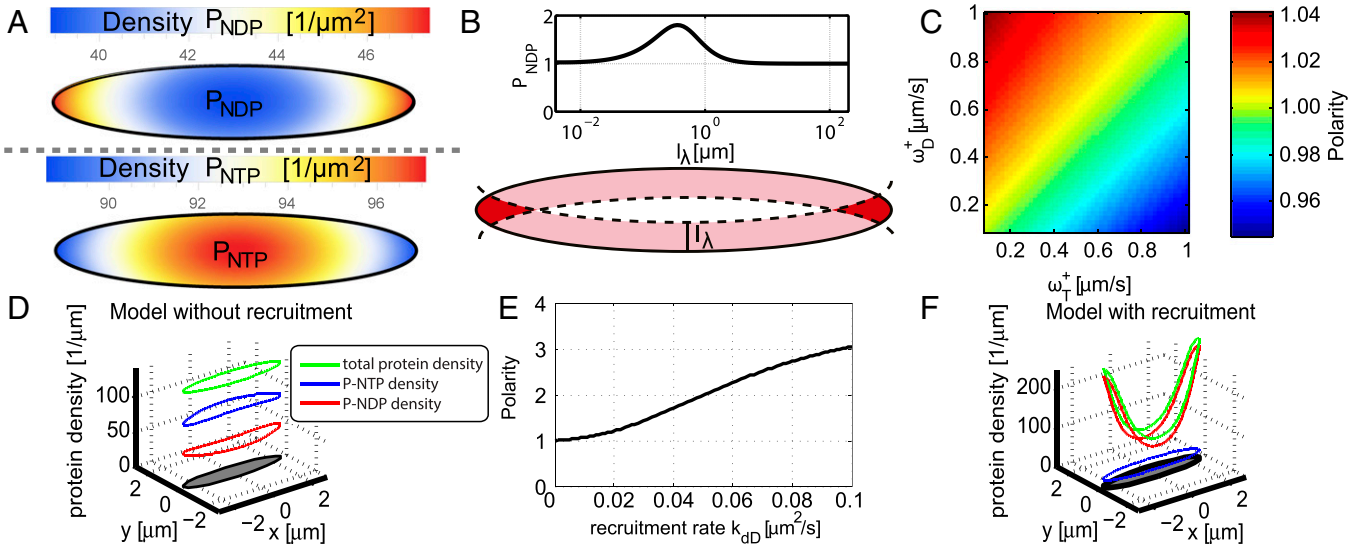

Fig. 2. Membrane affinity controls, and recruitment amplifies geometry adaption. The cells used for the numerical studies have a length of $L = 5$ μm and a width of $l = 1$ μm. (*A*) Even when recruitment is turned off, P_{NTP} and P_{NDP} form inhomogeneous density profiles in the cytosol. P_{NDP} accumulates close to the poles and is depleted at midcell. In contrast, P_{NTP} exhibits high concentration at midcell and a low concentration at the poles. The attachment and detachment rates are set to 1 μm/s and 1 s^{-1}, respectively, which gives a penetration depth $l_\lambda \approx 1.6$ μm. (*B*) Illustration of the source degradation mechanism for the spatial segregation of cytosolic P_{NDP} and P_{NTP}. All proteins that detach from the membrane are in an NDP-bound state and can undergo nucleotide exchange; the range of P_{NDP} in the cytosol is limited to a penetration depth l_λ (dashed lines); here, $l_\lambda = 0.35$ μm. At the poles, this reaction volume receives input from opposing faces of the membrane, resulting in an accumulation of cytosolic P_{NDP} (dark red). The magnitude of this accumulation depends on the penetration depth. The polarity $P_{NDP} = u_d^{pole}/u_d^{mid-cell}$ of membrane-bound P_{NDP} plotted as a function of l_λ shows a maximum at $l_\lambda \approx 0.35$ μm and vanishes in the limits of large as well as small penetration depths. (*C*) Polarity *P* of membrane-bound proteins as a function of the attachment rates, ω_D^+ and ω_T^+, with cooperative binding (recruitment) turned off. While for $\omega_D^+ > \omega_T^+$ membrane-bound proteins form a bipolar pattern ($P > 1$), they accumulate at midcell ($P < 1$) for $\omega_D^+ < \omega_T^+$. (*D*) Density profiles of membrane-bound proteins in the limit where the attachment rates of the two species are equal, $\omega_D^+ = \omega_T^+ = 1$ μm/s, and recruitment is switched off. The membrane profile of the total protein density (green) is flat, whereas membrane-bound P_{NTP} (blue) accumulates at midcell and P_{NDP} (red) forms a bipolar pattern. (*E*) Polarity *P* of the membrane-bound proteins as a function of k_{dD} for $\omega_D^+ = \omega_T^+$. Increasing the recruitment rate restores polarity. (*F*) Density profiles of membrane-bound proteins for the same parameter configuration as in *E* with $k_{dD} = 0.1$ $\mu m^2/s$. The density of P_{NDP} (red) as well as the overall protein density (green) exhibit strongly bipolar patterns, which are much more pronounced than the corresponding patterns in the absence of cooperative membrane binding. The density of P_{NTP} (blue) is comparatively flat, and there are much less membrane-bound proteins in this nucleotide state than in the P_{NDP} state. The overall protein pattern is strongly dominated by P_{NDP}.

two distinct types of pattern: membrane-bound proteins either accumulate at midcell or form a bipolar pattern with high densities at both cell poles. The polarity of these patterns is quantified by the ratio of the density of membrane-bound proteins located at the cell poles (u_{pole}) to that at midcell ($u_{midcell}$): $P = u_{pole}/u_{midcell}$. First, we investigated the impact of preferential recruitment of either P_{NTP} or P_{NDP} to the membrane, defined as $R = (k_{dD} - k_{tT})/(k_{dD} + k_{tT})$, on cell polarity. We find that proteins accumulate at the cell poles ($P > 1$) if there is a preference for cooperative binding of P_{NDP} ($R > 0$). Moreover, the polarity *P* of this bipolar pattern becomes more pronounced with increasing *R*. This scenario corresponds to the strongly bipolar pattern of AtMinD observed in mutant *E. coli* cells lacking EcMinD and EcMinE (18). In contrast, when cooperative binding favors P_{NTP} ($R < 0$), proteins accumulate at midcell ($P < 1$). Thus, the sign of the recruitment preference *R* for a protein in a particular nucleotide state controls the type, whereas its magnitude determines the amplitude of the pattern. Next, we investigated how cell geometry affects the pattern, while keeping *R* fixed. Upon varying the length of the long axis, *L*, while keeping the length of the short axis fixed at $l = 1$ μm, we find that the aspect ratio L/l controls the amplitude of the pattern, but leaves the type of pattern unchanged. With increasing eccentricity of the ellipse, the respective pattern becomes more sharply defined; for a spherical geometry, the pattern vanishes. In summary, cell geometry controls the definition of the pattern, and the preference for membrane recruitment of a certain nucleotide state determines the location on the cell membrane where the proteins accumulate and how pronounced this accumulation becomes.

Why Geometry Influences Patterning. Our finding that recruitment is a major determinant of cell polarity suggests that there is some underlying intrinsic affinity of the two protein species for either the cell poles or the midzone. This affinity cannot be encoded in the attachment or recruitment rates alone, because these are position independent. Instead, it must emerge from the interplay between these reactions, cell geometry, and diffusion. To uncover the underlying mechanism, we first performed a numerical study where we omitted all cooperative membrane binding processes, such that the dynamics became linear. Interestingly, we observed that, although the overall protein density is homogeneous in the cytosol (see *SI Appendix*), P_{NDP} and P_{NTP} are nevertheless spatially segregated, accumulating in the vicinity of the cell poles and close to midcell, respectively (Fig. 2*A*). This observation, the origin of which will be discussed later, explains how patterns of membrane-bound proteins arise: these inhomogeneities in protein densities in the cytosol serve as seeds for the polarization of the protein pattern on the membrane, and their respective impact is regulated by the attachment rates ω_D^+ and ω_T^+. The pattern of the protein species with the higher membrane affinity determines the type of the pattern (Fig. 2*C*). If P_{NDP} has the larger membrane affinity, a bipolar pattern emerges, whereas one observes enrichment of membrane-bound proteins at midcell if attachment of P_{NTP} dominates. Note that the detachment rates have the inverse effect (cf. *SI Appendix*).

Next, to analyze the additional nonlinear effects of membrane recruitment, we considered a situation, illustrated in Fig. 2*D*, where both nucleotide states have the same membrane affinity. As a result, the steady-state membrane density becomes uniform (see *SI Appendix*). Because cooperative membrane binding effectively increases the affinity of a protein species just like an

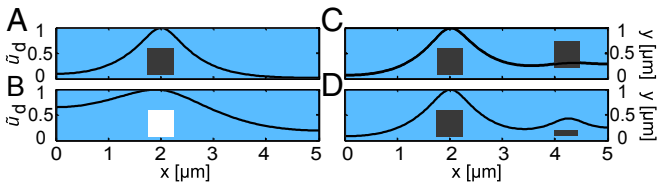

Fig. 3. Two-dimensional planar geometry with cytosolic volume (blue) above a membrane at $y = 0$. The left, right, and top boundaries of the cytosolic regime are reflecting boundaries. Diffusion and nucleotide exchange rates are set to their standard values, and the total number of proteins is set to $N = 50$. Black boxes indicate areas that are not accessible to the proteins and thereby generate excluded reaction volumes; the boundaries of the boxes are assumed to be reflecting. Solid curves show the normalized density of P_{NDP} bound to the membrane: $\tilde{u}_d = u_d / u_d^{max}$. Generally, P_{NDP} accumulates at membrane regions in the vicinity of the cytosolic areas with excluded reaction volumes, with the effect being stronger with larger excluded reaction volumes and closer to the membrane (*A*, *C*, and *D*). In *B*, the white box indicates that, within its volume, all proteins are allowed to diffuse, but they do not undergo nucleotide exchange. This has a similar but weaker effect to that observed in the other panels: the proteins accumulate at the membrane near the excluded reaction volume. The parameters used in these numerical experiments are summarized in *SI Appendix*, Table 1.

increase in the respective attachment rate, we expected that membrane patterns could be restored by switching the recruitment processes back on. Indeed, we found a strong increase in polarity upon raising the recruitment rate k_{dD} for fixed $k_{tT} = 0$ (Fig. 2*E*). Moreover, for large recruitment rates, not only does the relative level of the two species on the membrane change, but the pattern of P_{NDP} becomes highly polar (Fig. 2*F*). The reason is the positive feedback facilitated by cooperative membrane binding: in membrane regions facing a cytosolic region with an enhanced P_{NDP} concentration, binding leads to a locally increased concentration, which in turn increases the net attachment rate. Recruitment strongly amplifies the slight dominance of P_{NDP} already existing at the cell poles in the absence of cooperative membrane binding, and thereby leads to the observed strongly bipolar P_{NDP} membrane pattern.

In summary, the above analysis shows that the mechanism underlying the pattern-forming process is intrinsic to the protein dynamics: an inhomogeneous protein density in the cytosol together with unequal membrane affinities of the two forms leads to a spatially nonuniform accumulation of membrane-bound proteins. Nonlinear dynamics in the form of cooperative membrane binding (recruitment) serves to amplify these weakly nonuniform profiles into pronounced membrane patterns.

Cytosolic Reaction Volume Determines the Pattern. After investigating the phenomenology of geometry-dependent pattern formation, we were left with the key question: what is the origin of the observed spatial segregation of P_{NTP} and P_{NDP} in the cytosol? Because these patterns form without cooperative membrane binding, the mechanism must be based on the combined effect of membrane attachment and detachment, diffusion, and nucleotide exchange. Moreover, as all chemical processes are spatially uniform, the key to understanding the impact of cell geometry must lie in the diffusive coupling of these biochemical processes.

Consider the situation where the attachment rates for P_{NDP} and P_{NTP} are equal, such that the total protein density on the membrane becomes spatially homogeneous (Fig. 2*D*). Only P_{NDP} is released from the membrane. Hence, the latter acts as a source of cytosolic P_{NDP}. Because, in addition, cytosolic P_{NDP} is transformed into cytosolic P_{NTP} by nucleotide exchange, we have all of the elements of a source degradation process. The ensuing density profile for P_{NDP} in the cytosol is exponential with the decay length set by $l_\lambda = \sqrt{D_c/\lambda}$. Due to membrane curvature these reaction volumes overlap close to the cell poles (Fig. 2*B*, *Bottom*), which implies an accumulation of P_{NDP} at the cell poles. The effect becomes stronger with increasing membrane curvature. Moreover, there is an optimal value for the penetration depth l_λ, roughly equal to a third of the length l of the short cell axis, that maximizes accumulation of P_{NDP} at the cell poles (Fig. 2*B*, *Top*). As l_λ becomes larger than l, the effect weakens, because the reaction volumes from opposite membrane sites also overlap at midcell. In the limit where l_λ is much smaller than the membrane curvature at the poles, the overlap vanishes, and with it the accumulation of P_{NDP} at the poles.

Expressed differently, these heuristic arguments imply that the local ratio of the reaction volume for nucleotide exchange to the available membrane surface is the factor that explains the dependence of the protein distribution on cell geometry. To put this hypothesis to the test, we performed numerical simulations that are in the spirit of a minimal system approach taken by in vitro experiments (23, 25). In our numerical setup, we considered a cytosolic volume adjacent to a flat membrane, as illustrated in Fig. 3. We were interested in how alterations in the volume of cytosol available for protein diffusion and/or nucleotide exchange would affect the density profile on the membrane.

In accordance with our hypothesis, we find that excluding volume for diffusion in the vicinity of a flat membrane reduces the available reaction volume locally and leads to accumulation of proteins at the membrane (Fig. 3 *A*, *C*, and *D*). The larger the excluded volume, the more proteins accumulated at the membrane. To focus on reaction volume explicitly, we considered a situation in which nucleotide exchange was disabled in a given region of the cytosolic area but proteins could still diffuse in and out of it. Again, we found protein accumulation at the nearby membrane but with reduced amplitude (Fig. 3*B*). Hence, these numerical studies strongly support our heuristic arguments and lead us to conclude that it is indeed exclusion of the reaction volume for nucleotide exchange that provides for the adaptation of the pattern to the geometry of the setup. Likewise, the membrane patterning in a cell could be effected by the nucleoid if the DNA material acts as a diffusion barrier, although at present this is debated (26). In the *SI Appendix*, we study how different sizes of effective excluded volume change the membrane pattern. Although bipolarity is still obtained for a broad parameter range, the complex geometry gives rise to a richer spectrum of possible patterns: for large sizes of excluded volume, accumulation at the poles occurs for $R < 0$ (preferential recruitment for P_{NTP}), whereas for $R > 0$ the proteins accumulate at midcell. For intermediate sizes, there are parameter ranges where patterns with several maxima, not necessarily at the poles or midcell, are observed.

Pattern Formation Does Not Require a Dynamical Instability. The above analysis shows that the difference in local reaction volume for cytosolic nucleotide exchange is the key element of the mechanism underlying geometry sensing. To put this result in perspective with pattern formation mechanisms based on dynamical instabilities, we consolidated the key properties of the spatially extended model in a spatially discretized version amenable to rigorous analytical treatment (Fig. 4*A*).

Diffusion in the cytosol and on the membrane is treated in terms of exchange processes between a network of nodes. A minimal set comprises four nodes on the membrane, two at the poles and two at midcell, and a distribution of nodes in the cytosol, which ensures that the ratio of membrane area to bulk volume at the cell poles is higher than at midcell. Because all observed stationary patterns are symmetrical with respect to both symmetry axes, we can further reduce the network to one quadrant of the ellipse (Fig. 4*B*). We are now left with a network of one membrane node at a pole and one at midcell, two nodes serving as the interface between membrane and cytosol, and three cytosolic nodes whose distribution reflects the asymmetry in the cytosolic reaction volume between the cell poles and midcell.

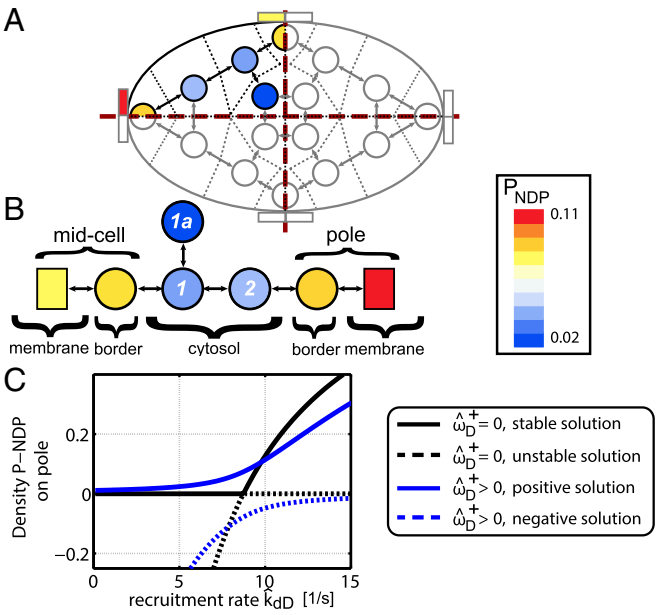

Fig. 4. Reduced network model and bifurcation analysis. (*A*) The full spatiotemporal dynamics in an ellipse is reduced to the nonlinear dynamics of a network of coupled nodes. We take the minimal possible number of nodes reflecting the asymmetry in the ratio of membrane area to bulk volume at the cell poles and midcell. Diffusion in the cytosol is modeled as particle exchange processes between the nodes. The network equations are derived from a discrete time jump process. Because the symmetry of the pattern reflects the symmetry of the ellipse, there is no flux of particles through either midplanes (red dashed lines). Therefore, the network can be further reduced to a single quadrant (black) with the other quadrants (gray) simply mirroring its behavior. (*B*) The reduced model comprises two membrane nodes at the pole and at midcell, two border nodes connecting membrane and cytosol, as well as three cytosolic nodes. Node 1*a* captures the increased ratio of membrane area to bulk volume at midcell. As illustrated by the colored nodes, this minimal network model polarizes: the density of P_{NDP} at the pole node is higher than on the membrane node. (*C*) Density of P_{NDP} at the pole node as a function of the recruitment rate $\hat{k}_{dD}$. The density is given relative to the total number of particles located at the membrane node of the pole. For vanishing attachment rate of P_{NDP}, $\hat{\omega}_D^+ = 0$, there is a transcritical bifurcation at a critical rate $\hat{k}_{dD}^* \approx 8.7\ s^{-1}$ where a polarized state exchanges stability with an unpolarized state (black lines). In contrast, for the generic case of finite membrane attachment, $\hat{\omega}_D^+ > 0$, there is only one positive fixed-point solution that is always stable (blue lines).

We have analyzed the ensuing mathematical model, a system of coupled ordinary differential equations, in the context of dynamic systems theory; for mathematical details and the model parameters used, please refer to the *SI Appendix*. Confirming our previous reasoning, we found that the reduced network model indeed leads to polarization between cell pole and midcell (Fig. 4*B*). Moreover, from a bifurcation analysis, we learn that generically the dynamic system does not exhibit a bifurcation: there is only one physically possible solution with positive protein density on the membrane, and this density increases with the recruitment rate (Fig. 4*C*). Only in the special (nongeneric) case where the attachment rate of P_{NDP} vanishes, $\hat{\omega}_D^+ = 0$, do we find a transcritical bifurcation. Then, there is a critical recruitment rate $\hat{k}_{dD}^*$ below which the membrane is depleted of P_{NDP}. In other words, generically the system shows an imperfect transcritical bifurcation, which implies robustness of the mechanism linking protein distribution to cell geometry.

Discussion

How does protein patterning adapt to cell geometry? Dynamic models for pattern formation often reduce the cytosolic volume to the same dimension as the membrane and focus on the role of nonlinear protein interactions (see, e.g., refs. 11 and 27). At first sight, this appears to make sense, because diffusion coefficients are generically much higher in the cytosol than on the membrane. Indeed, if only attachment and detachment processes are involved, any transient geometry-dependent pattern is rapidly washed out (17).

Here, we have shown that the assumption of a well-mixed cytosolic protein reservoir becomes invalid as soon as cytosolic processes like nucleotide exchange, which alter protein states, become involved. We have introduced a minimal reaction module with a single NTPase that cycles between membrane and cytosol. The fact that cytosolic nucleotide exchange may take place on a diffusive length scale far below cell size has been noted previously (13), and it has been shown that this can be critical for robust, intracellular pattern formation (15). Our analysis reveals that nucleotide exchange leads to an inhomogeneous protein distribution in the cytosol, which is stably maintained and depends strongly on the geometry of the cytosolic space. As a consequence, proteins accumulate on certain membrane regions, depending on the local ratio of membrane area to cytosolic volume. In an elongated cell, this serves as a robust mechanism for proper cell division by facilitating protein accumulation at the poles. The proposed reaction module operates through implicit curvature sensing and does not require that the relevant protein themselves respond to membrane curvature (7, 9) or lipids (28). The degree and the axis of polarization depend on the level of cooperativity in membrane binding, which can be regulated by enzymes.

Our theoretical analysis suggests that evolutionary tuning of this simple reaction module is feasible: because there is no threshold involved, polarity can be improved continuously starting from any parameter configuration. This lack of a threshold can at the same time also be a disadvantage: without a trigger, pattern formation is difficult to induce as response to an upstream event. Another distinctive element of the mechanism is the lack of a characteristic length scale (e.g., as striped Min patterns in *E. coli*); instead, the pattern scales with the size of the cell. Depending on the functional role, this might be desired or disadvantageous.

The reaction module gives a possible explanation for the bipolar patterns of AtMinD observed in mutant *E. coli* cells (18). Several experimental tests could be performed to validate the proposed reaction module: one route would be to study spherical *E. coli* cells. For this geometry, we predict that the polarization of AtMinD should vanish, because the membrane curvature is uniform. This, however, would also be the case if the kinetics of AtMinD binding is directly dependent on membrane curvature, as in the case of DivIVa (7, 9). To rule out this scenario, an in vitro experiment could be conducted, as described in Fig. 3.

In vitro experiments might also serve as a proof of concept for the use of the suggested reaction module in nanoscale self-organization. By enzymatically regulating the kinetic rates of the process, one could induce protein patterns on a membrane, which then serve as templates for the localization of nanoscale structures, e.g., similar to the formation of actin cables close to Cdc42 protein caps in yeast. Localization could either be self-organized or target specific curvatures or be externally controlled by volume exclusion in the cytosolic space. If, in addition, such nanostructures exert forces on the membrane, this self-organization principle could be used to regulate the shape of membranes. Thus, the proposed minimal module might serve as a core network for the design of other geometry-sensing protein networks.

On a more speculative note, geometry-sensing protein networks like the one discussed here would enable a cell to gradually optimize its biological function, because the underlying mechanism does not involve a bifurcation threshold. For example, one could envision a biochemical network containing a protein that is able to trigger hydrolysis-driven detachment. Such

a catalytic process could act selectively on the P_{NTP} or the P_{NDP} species. This would create an imbalance between the effective membrane affinities of P_{NTP} and P_{NDP}, and thus regulate polarity. Moreover, the copy number of such a catalyst would become an evolutionary tunable modulator of the effective imbalance. MinE in *E. coli*, which stimulates the hydrolysis of membrane-bound MinD-ATP, is a possible instance of such a factor.

Finally, due to its generic nature, the proposed mechanism might be involved in many bacterial pattern-forming systems. For instance, the sensitivity to cytosolic reaction volume provides a way to sense large cytosolic structures. This could, for instance, be part of the mechanism that guides PomZ to midcell in *Myxococcus xanthus* (29). One could also imagine direct feedback mechanisms between force-exerting proteins that regulate cell shape (e.g., FtsZ ring contraction) and proteins that adapt to local cell shape by sensing the local reaction volume, and which guide the downstream accumulation of further force-exerting proteins. In this scenario, cell shape could be controlled (even in a self-organized fashion) by balancing these two processes.

Materials and Methods

The model is mathematically described as a set of reaction–diffusion equations (*SI Appendix*). All simulations were performed with finite-element methods on a triangular mesh using Comsol Multiphysics 4.3. As initial condition, all proteins were in the NDP state and located in the bulk of the ellipse. In Fig. 3, the particles are initially located on the membrane in the NDP state. For Figs. 1 and 2, the simulation time was 1,000 s, and for Fig. 3, it was 2,000 s. A steady state is reached after ∼100 s.

ACKNOWLEDGMENTS. This research was supported by the German Excellence Initiative via the program "NanoSystems Initiative Munich," and the Deutsche Forschungsgemeinschaft via Project B02 within the SFB 1032 "Nanoagents for Spatio-Temporal Control of Molecular and Cellular Reactions."

1. Ephrussi A, St Johnston D (2004) Seeing is believing: The bicoid morphogen gradient matures. *Cell* 116(2):143–152.
2. Wedlich-Söldner R, Altschuler S, Wu L, Li R (2003) Spontaneous cell polarization through actomyosin-based delivery of the Cdc42 GTPase. *Science* 299(5610): 1231–1235.
3. Klünder B, Freisinger T, Wedlich-Söldner R, Frey E (2013) GDI-mediated cell polarization in yeast provides precise spatial and temporal control of Cdc42 signaling. *PLoS Comput Biol* 9(12):e1003396.
4. Lutkenhaus J (2007) Assembly dynamics of the bacterial MinCDE system and spatial regulation of the Z ring. *Annu Rev Biochem* 76:539–562.
5. Raskin DM, de Boer PA (1999) Rapid pole-to-pole oscillation of a protein required for directing division to the middle of *Escherichia coli*. *Proc Natl Acad Sci USA* 96(9):4971–4976.
6. Hu Z, Gogol EP, Lutkenhaus J (2002) Dynamic assembly of MinD on phospholipid vesicles regulated by ATP and MinE. *Proc Natl Acad Sci USA* 99(10):6761–6766.
7. Strahl H, Hamoen LW (2012) Finding the corners in a cell. *Curr Opin Microbiol* 15(6): 731–736.
8. Zamparo M, et al. (2015) Dynamic membrane patterning, signal localization and polarity in living cells. *Soft Matter* 11(5):838–849.
9. Lenarcic R, et al. (2009) Localisation of DivIVA by targeting to negatively curved membranes. *EMBO J* 28(15):2272–2282.
10. Meinhardt H, de Boer PA (2001) Pattern formation in *Escherichia coli*: A model for the pole-to-pole oscillations of Min proteins and the localization of the division site. *Proc Natl Acad Sci USA* 98(25):14202–14207.
11. Howard M, Rutenberg AD, de Vet S (2001) Dynamic compartmentalization of bacteria: Accurate division in *E. coli*. *Phys Rev Lett* 87(27 Pt 1):278102.
12. Meacci G, Kruse K (2005) Min-oscillations in *Escherichia coli* induced by interactions of membrane-bound proteins. *Phys Biol* 2(2):89–97.
13. Huang KC, Meir Y, Wingreen NS (2003) Dynamic structures in *Escherichia coli*: Spontaneous formation of MinE rings and MinD polar zones. *Proc Natl Acad Sci USA* 100(22):12724–12728.
14. Varma A, Huang KC, Young KD (2008) The Min system as a general cell geometry detection mechanism: Branch lengths in Y-shaped *Escherichia coli* cells affect Min oscillation patterns and division dynamics. *J Bacteriol* 190(6):2106–2117.
15. Halatek J, Frey E (2012) Highly canalized MinD transfer and MinE sequestration explain the origin of robust MinCDE-protein dynamics. *Cell Reports* 1(6):741–752.
16. Fange D, Elf J (2006) Noise-induced Min phenotypes in *E. coli*. *PLoS Comput Biol* 2(6):e80.
17. Rangamani P, et al. (2013) Decoding information in cell shape. *Cell* 154(6):1356–1369.
18. Zhang M, Hu Y, Jia J, Gao H, He Y (2009) A plant MinD homologue rescues *Escherichia coli* HL1 mutant (DeltaMinDE) in the absence of MinE. *BMC Microbiol* 9(1):101.
19. Aldridge C, Møller SG (2005) The plastid division protein AtMinD1 is a Ca^{2+}-ATPase stimulated by AtMinE1. *J Biol Chem* 280(36):31673–31678.
20. Zhou H, et al. (2005) Analysis of MinD mutations reveals residues required for MinE stimulation of the MinD ATPase and residues required for MinC interaction. *J Bacteriol* 187(2):629–638.
21. Fujiwara MT, et al. (2004) Chloroplast division site placement requires dimerization of the ARC11/AtMinD1 protein in *Arabidopsis*. *J Cell Sci* 117(Pt 11):2399–2410.
22. Meacci G, et al. (2006) Mobility of Min-proteins in *Escherichia coli* measured by fluorescence correlation spectroscopy. *Phys Biol* 3(4):255–263.
23. Loose M, Fischer-Friedrich E, Herold C, Kruse K, Schwille P (2011) Min protein patterns emerge from rapid rebinding and membrane interaction of MinE. *Nat Struct Mol Biol* 18(5):577–583.
24. Shih YL, Fu X, King GF, Le T, Rothfield L (2002) Division site placement in *E. coli*: Mutations that prevent formation of the MinE ring lead to loss of the normal midcell arrest of growth of polar MinD membrane domains. *EMBO J* 21(13):3347–3357.
25. Loose M, Mitchison TJ (2014) The bacterial cell division proteins FtsA and FtsZ self-organize into dynamic cytoskeletal patterns. *Nat Cell Biol* 16(1):38–46.
26. Sanamrad A, et al. (2014) Single-particle tracking reveals that free ribosomal subunits are not excluded from the *Escherichia coli* nucleoid. *Proc Natl Acad Sci USA* 111(31): 11413–11418.
27. Alonso S, Bär M (2010) Phase separation and bistability in a three-dimensional model for protein domain formation at biomembranes. *Phys Biol* 7(4):046012.
28. Huang KC, Mukhopadhyay R, Wingreen NS (2006) A curvature-mediated mechanism for localization of lipids to bacterial poles. *PLoS Comput Biol* 2(11):e151.
29. Treuner-Lange A, Søgaard-Andersen L (2014) Regulation of cell polarity in bacteria. *J Cell Biol* 206(1):7–17.